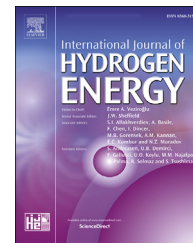




ELSEVIER

Available online at www.sciencedirect.com

ScienceDirect

journal homepage: www.elsevier.com/locate/he

A comparative study on the microstructure and cycling stability of the amorphous and nanocrystallization $Mg_{60}Ni_{20}La_{10}$ alloys

Yiming Li, Zhuocheng Liu, Yanghuan Zhang, Huiping Ren*

Key Laboratory of Integrated Exploitation of Bayan Obo Multi-Metal Resources, Inner Mongolia University of Science and Technology, Baotou 014010, China

ARTICLE INFO

Article history:

Received 29 May 2018

Received in revised form

3 August 2018

Accepted 9 August 2018

Available online xxx

Keywords:

Mg based hydrogen storage alloys

Nanocrystallization

Microstructural stabilization

Cycling stability

ABSTRACT

Amorphous and nanocrystalline $Mg_{60}Ni_{20}La_{10}$ alloys were prepared by melt-spun and crystallization of the amorphous alloy respectively. Microstructural evolution of the amorphous and crystallized (CA) alloys during hydrogenation/dehydrogenation cycles was studied and compared in the present work. The CA alloy exhibits homogeneous and fine (<50 nm) multiphase microstructure composed of $LaMg_2Ni$, Mg_2Ni and $LaMgNi_4$. The CA alloy has slightly lower hydrogenation ability but far excellent cycling stability compared with the amorphous alloy. The amorphous and CA alloys have identical phase constitution including Mg_2Ni and LaH_3 after cycling. While, microstructures of the two cycled alloys show dramatically distinct characters. Grain size of the cycled CA alloy is almost unchanged compared with the original alloy, which contributes to the better cycling stability. However, grain growth especially coarsening of Mg_2Ni is severe in the cycled amorphous alloy, leading to difficulty to dehydrogenation. The better coarsening resistance of the CA alloy is attributed to the crisscrossed distribution of Mg_2Ni and LaH_3 and well-matched interfacial configuration between Mg_2Ni and LaH_3 that $(113)Mg_2Ni$ $(111)LaH_3$. However, hydrogenation of the amorphous alloy leads to large and inhomogeneous microstructure which is ascribed to the preferential recrystallization and growth of Mg_2Ni , contributing to rapid degradation of the amorphous alloy. The present work illumines a potential way to prepare stable nanocrystalline by introducing secondary phase with interlaced microstructure and well-matched interfacial configuration using nanocrystallization method.

© 2018 Hydrogen Energy Publications LLC. Published by Elsevier Ltd. All rights reserved.

Introduction

Mg-based alloys which are proposed as the most promising candidates for hydrogen storage have been received significant concerns for decays [1,2]. However, the stable thermodynamics and sluggish kinetics upon hydrogenation/

dehydrogenation are of the significant bottleneck for the practical applications of Mg-based alloys [1–3]. In order to overcome these problems, several strategies including alloying, catalysis, amorphization, nanoscaling etc. have been adopted and intensively investigated in the recent years [1–5]. Among these methods, nanocrystalline is demonstrated to be an effect way for improvement of the hydrogen storage

* Corresponding author.

E-mail address: renhuiping@sina.com (H. Ren).<https://doi.org/10.1016/j.ijhydene.2018.08.129>

0360-3199/© 2018 Hydrogen Energy Publications LLC. Published by Elsevier Ltd. All rights reserved.

performances due to the ultra-fine microstructure and large number of grain boundaries [3–5]. Although nanocrystalline Mg-based alloys present improved hydrogen storage performance, the hydrogen absorption capacity and kinetics deteriorate rapidly which is mainly caused by grain coarsening during the long term hydrogenation/dehydrogenation cycles [3–6]. Thus, microstructural stabilization is the key issue for development of the nanocrystalline Mg-based hydrogen storage alloys.

Nanocrystalline alloys can be prepared by ball milling, hydriding combustion, melt spinning, thin film technology and chemical synthesis etc. [6–10]. Besides, crystallization of the amorphous alloys is confirmed to be an effective way to prepare the nanocrystalline materials [11,40]. In the Mg-based system, Mg–Ni–RE alloys have received tremendous attentions due to the excellent performances for both gaseous [12–17] and electrochemical application [18–21]. The previous work found that adding of RE into the Mg–Ni alloys can dramatically improve the glass forming ability and hydrogenation performances [22]. Furthermore, nanocrystalline Mg–Ni–RE alloys with grain size of no more than 100 nm can be readily obtained by crystallization from the amorphous precursor [12–17]. And the nanostructure fabricated by nanocrystallization has been reported to be rather stable during the hydrogenation/dehydrogenation process. For example, nanocrystalline Mg₇₅Ni₂₅ alloy prepared by melt-spun and crystallization is almost unchanged after 5th absorption/desorption cycles [12]. Nanocrystallized Mg₉₀Ni₈RE₂ alloy keeps the nanostructure well after 23 gaseous cyclings [16]. Nanostructure of the crystallized Mg₈₅Ni₁₀La₅ alloy is very stable at the temperature below 300 °C [17]. Stability of the nanocrystalline is closely related to the grain size, phase constitution and micro-morphology [4,5]. However, in-depth know of relationship between the microstructural stability and nanocrystalline structure is still unclear.

In the present work, Mg₂Ni-type nanocrystalline Mg₆₀Ni₂₀La₁₀ alloy was prepared by melt-spun and followed by crystallization annealing. Microstructure evolution of the amorphous and crystallized alloys (hereinafter referred to as CA alloy) during the hydrogenation/dehydrogenation process was systematically studied and compared by XRD and TEM. Mechanism of the cycling stability corresponding with the microstructural characters was discussed.

Experimental materials and methods

The master Mg₆₀Ni₂₀La₁₀ alloy was prepared by induction levitation melting in a water-cooled copper crucible under helium atmosphere. La–Ni master alloy was firstly melted three times using raw metal, then Mg was adopted and remelted twice for homogeneity. Appropriate excess of Mg was added in order to compensate for the evaporative loss of Mg during melting. The as-cast alloy was remelted and spun on a rotating copper roller with a linear speed of 20 m s⁻¹. Crystallization of the melt-spun alloys was applied at certain temperature with a heating speed of 100 °C min⁻¹ in vacuum.

Crystal structure of the alloys was measured by Bruker-D8 Advance X-ray diffractometer (XRD). The microstructural and crystallographic information were also measured by

transmission electron microscopy (TEM: JEM-2100). High-Angle Annular Dark Field (HAADF) STEM image and EDS mapping analysis were performed by JEM-2100F. Samples for TEM analysis were ultrasonic dispersed of the fine powder in ethanol for 1800 s and then dropped into a carbon membrane support on the copper grid. High resolution TEM (HRTEM) images and corresponding diffraction patterns were reprocessed by fast Fourier transformation (FFT) using GMS program (GATAN). Thermal analysis of the as-spun alloy was studied by differential scanning calorimetric (DSC) using NETZSCH STA449F3 thermal analyzer at heating rate of 10 K min⁻¹ in argon atmosphere.

The hydrogen storage properties and hydrogenation cycling of the alloys were measured by Setaram-PCTPRO system using the Sievert's method. Before the measurement, the samples were pumped at 100 °C for 2 h. Each hydrogenation/dehydrogenation cycle consists of absorption at 2 MPa for 1–3 h and desorption by evacuating for 2 h at 250 °C.

Results and discussions

Microstructure and hydrogen storage performances of the amorphous and crystallized alloys

XRD and selected area electron diffraction (SAED) of the as-spun alloy are displayed in Fig. 1. The halo patterns in both XRD and SAED indicate the amorphous nature of the as-spun alloy. To identify the crystallization temperature of the as-spun alloy, DSC test was applied and the result is also shown in Fig. 1. Two exothermic peaks at 204 and 296 °C present in the DSC curve, indicating that the amorphous alloy crystallizes in two steps. From the DSC result, crystallization of the as-spun alloy was handled at 310 °C for 1 h.

Fig. 2 is XRD profile of the crystallized (CA) alloy, in which sharp peaks are evident indicating formation of the crystal state. Three structures including LaMg₂Ni, Mg₂Ni and LaMgNi₄ can be identified in the XRD pattern. The structural parameters and phase abundance are refined and recalculated by Rietveld method using Maud program. The calculated profile is in good accordance with the measured pattern as also shown in Fig. 2, and the detailed data is listed in Table 1.

To comprehend microstructure of the CA alloy further, TEM observation was adopted and the results are given in Fig. 3. From the bright field (BF) images of the CA alloy (see in Fig. 3(a and b)), it is obvious that crystallization of the amorphous Mg₆₀Ni₂₀La₁₀ alloy leads to rather homogeneous nanostructure with the grain size less than 50 nm. SAED (Fig. 3(c)) of the CA alloy presents diffraction rings which are the typical diffraction pattern of nanostructure materials. Indexing of these diffraction rings agrees well with the result of XRD that LaMg₂Ni, Mg₂Ni and LaMgNi₄ exist in the CA alloy.

Furthermore, high resolution TEM (HRTEM) images of the CA alloy are shown in Fig. 4. LaMg₂Ni, Mg₂Ni and LaMgNi₄ can also be ascertained by the corresponding interplanar distances and fast Fourier transformation (FFT) diffraction patterns, as shown in Fig. 4(a–c). A LaMgNi₄ grain exhibits triangular shape which is similar with that of nano-YMgNi₄ grains in a nanocrystallization Mg₁₁Y₂Ni₂ alloy [23]. In general,

Download English Version:

<https://daneshyari.com/en/article/11011658>

Download Persian Version:

<https://daneshyari.com/article/11011658>

[Daneshyari.com](https://daneshyari.com)